第483回電波研連F分科会
開催日：2004年4月23日

Spatio-Temporal Characterization of Line-of-Sight and Room-to-Room Propagation in Home Environments with Ultra Wideband Signal

Katsuyuki Haneda†, Jun-ichi Takada† and Takehiko Kobayashi‡
UWB Technology Institute, National Institute of Information and Communications Technology,
3–4, Hikarino-oka, Yokosuka-city, Kanagawa, 239–0847 JAPAN
†Tokyo Institute of Technology, ‡Tokyo Denki University
Email: haneda@ap.ide.titech.ac.jp

***Abstract*— In this paper, spatio-temporal analysis of LOS and NLOS home environments based on the deterministic approach are presented. The detected paths were classified into several clusters by a heuristic approach. The identified clusters were determined from the physical structures of the environment, i.e. room height, specular directions and size of scatterers in both LOS and NLOS case, which means that the spatial and temporal channel characteristics are highly correlated. The NLOS environment was more diffuse than the LOS channel and the power propagating over the NLOS channel tends to be more distributed around the specular directions than the LOS case, due to the wall which separates the Tx and Rx. Intra-cluster properties were derived based on the moment analysis, instead of deriving a probability density function (PDF) within the cluster. The residual power spectrum after the extraction of 100 deterministic components were identified as diffuse components and their characteristics were discussed.**

I. Introduction

Ultra Wideband (UWB) is thought of as one of the candidates to realize future high data rate communications. It is assumed to be implemented mainly for indoor environments, but its system performance can suffer from dense multipath propagation. In order to construct an efficient UWB system, detailed investigations of the propagation channels are crucial. We have already proposed a frequency domain channel estimation scheme in a deterministic way which achieves high resolution with a UWB signal [1], [2]. In this paper, results of spatio-temporal channel characterization in a typical home environment in Japan are presented. First, separation of deterministic components and diffuse components [3] were examined. After that, clusterization of deterministic components was conducted along with the investigations of its intra-cluster properties and relation to physical phenomena. For the diffuse components, several qualitative observations are given.

II. Channel Estimation System

The channel estimation system consists of a data measurement process and derivation of channel parameters. In the measurement, transfer functions were extracted by a Vector Network Analyzer (VNA) along with a X-Y scanner and a X-stage with a single wideband antenna which realizes the synthesized antenna aperture in both sides of the link [4]. The structure of the measurement system is depicted in Fig. 1. The spatially sampled transfer functions are then applied to the Maximum Likelihood based estimator, SAGE. Conventionally

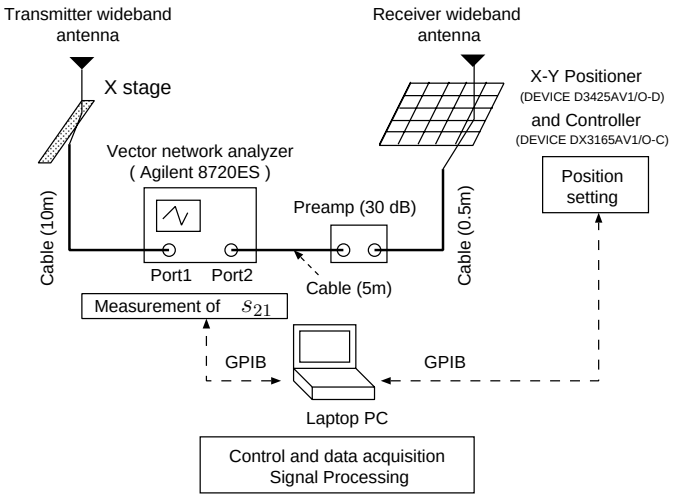

Fig. 1. UWB channel sounding system [1], [2].

the algorithm is used for wideband channel estimation, but we modified it for UWB signals [1]. The algorithm is based on the deterministic approach of propagation channel characterization and estimates parameters and spectrum of each ray path. Spherical wave array mode vector was used for the wave incident model, which seemed to be more realistic in indoor wave propagation [2]. The SAGE was implemented with the Successive Interference Cancellation (SIC) manner, i.e., the estimated components were removed after the determination of wave parameters. This process was continued until the number of waves reached a predefined number or when the extracted spectrum was below the noise level. The double directional channel measurement enables us to deconvolve antenna transfer functions in both Tx and Rx sides which leads to the construction of antenna-independent channel models. Foremost in the parameters estimation process, we estimated the direction-of-arrival (DOA) and time-of-arrival (TOA) simultaneously. After that, direction-of-departure (DOD) estimation was carried out in which TOA was used for the gating of the transfer function. By using this implementation, the computational burden can be significantly reduced [4].

TABLE I

SPECIFICATIONS OF THE EXPERIMENT.

Bandwidth	3.1 to 10.6 GHz [5].
Frequency sweeping points	801.
Spatial sampling	Rx: 10 × 10 points in horizontal plane whose element spacing is 48 mm (less than half wavelength in 3.1 GHz). Tx: 10 points with 48 mm spacing.
Estimated parameters	DOA azimuth, elevation angle, DOD azimuth angle, delay time and spectrum.
Antennas	UWB monopole antennas [6].
Polarization	Vertical–Vertical.
Calibration	Function of VNA and back-to-back.
IF bandwidth of VNA	100 Hz.
SNR at the receiver	About 30 dB.

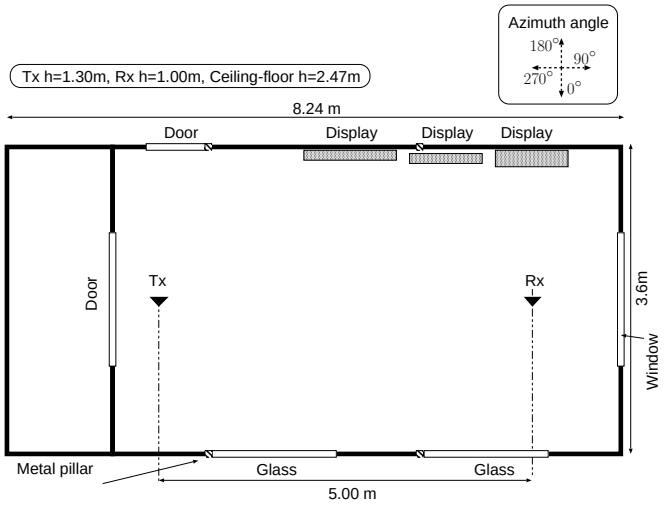

(a) LOS environment (1st floor of the house).

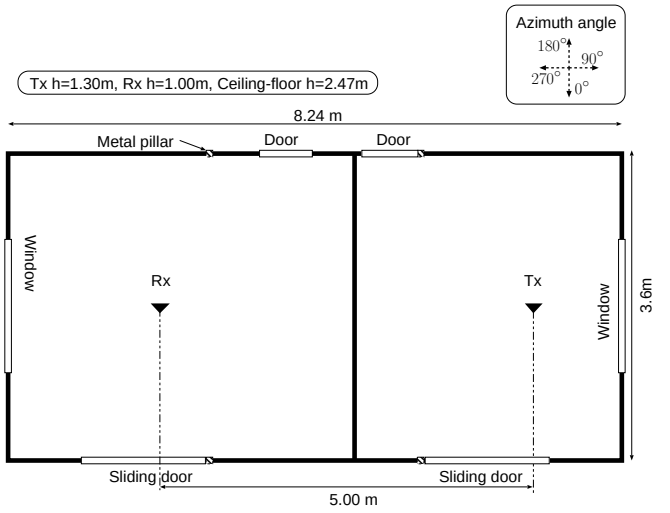

(b) NLOS environment (2nd floor of the house).

Fig. 2. Floor plan of the measurement environment.

III. LINE-OF-SIGHT CHANNEL MEASUREMENT

A. Experimental Setup

We conducted an experiment in a typical home environment in Japan. First, we evaluated a line-of-sight environment whose floor plan is depicted in Fig 2(a). In the measurement, element spacing of the synthesized array was set to 48 mm, which was equivalent to 0.49λ in the lowest frequency. The spatial resolution of our system was previously assessed in an anechoic chamber and 10 deg angle resolution was confirmed with the considered antenna aperture size. For the temporal resolution, 0.67 ns (20 cm) different two waves were accurately resolved with a 7.5 GHz bandwidth, which was the same in this experiment [2]. The bandwidth of the subband in the SAGE algorithm was 4 GHz. Antennas used were UWB monopole antennas whose fluctuation of group delay were less than 0.1 ns in the considered bandwidth [6]. Specifications of the experiment are shown in Table I. There was no furniture equipped in the room other than TV displays and small desks which were placed near the wall.

B. Separation of the Deterministic and Diffuse Components

With the mentioned channel sounding system, we detected 100 waves and regard them as deterministic components while the residual components were determined as a diffuse scattering. Although there is no concrete criteria to distinguish the deterministic and the diffuse components, the detected power of the deterministic components approached a floor level when the SIC detection of the SAGE went to 100 waves, then we can recognize the residual components as diffuse. As a result, the deterministic components consists of 70.24 % of the whole received power and 29.76 % still remains unextracted by SAGE. When both components were evaluated in a DOA azimuth-delay map, Fig. 3 was obtained. The upper figure shows the deterministic components, while the power spectrum of the diffuse components is shown in the lower figure as a contour plot. Note that initial results of this measurement including path identifications are covered in [4].

C. Clusterization of the Deterministic Components

On the azimuth-delay map, clusterization of the deterministic components were examined so that the whole detected paths were classified into 5 clusters as shown in Fig. 3(a). Among them, there are 2 to 3 sub-clusters observed in clusters A and E, which are expressed in red lines. Note that clusterization was done intuitively by a heuristic approach. From this figure, it can be concluded that the spatial and temporal characteristics are highly correlated in this channel.

In more detail, it was found that each cluster can be determined by physical structures of the environment, that is, specular direction, position and size of reflection objects. In

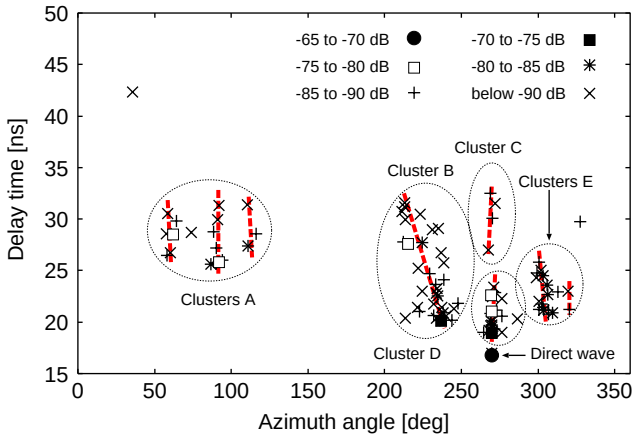

(a) Deterministic components estimated by SAGE and their clusterization.

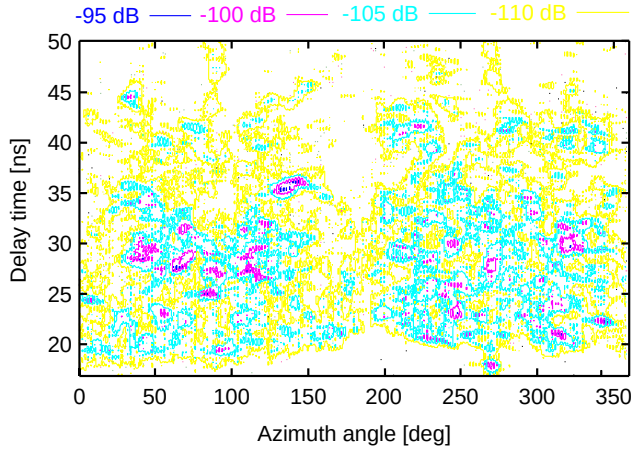

(b) Residual spectrum after the extraction of 100 waves.

Fig. 3. Separation of the deterministic components and diffuse components for LOS channel measurement.

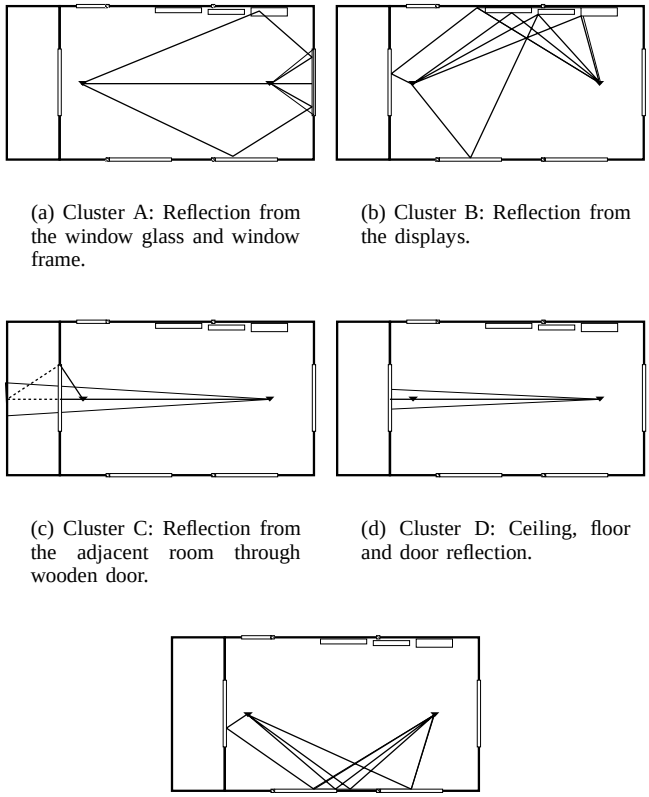

(a) Cluster A: Reflection from the window glass and window frame.

(b) Cluster B: Reflection from the displays.

(c) Cluster C: Reflection from the adjacent room through wooden door.

(d) Cluster D: Ceiling, floor and door reflection.

(e) Cluster E: Reflection from the window glass and window frame.

Fig. 4. Cluster identification with respect to physical structures of the environment for the LOS channel measurement. Typical paths are also shown.

Fig. 4, typical paths belonging to the clusters are shown on the floor plan. The shadowed regions correspond to the angle ranges of the incoming signals. Cluster A contains 3 sub-clusters, which represent the window reflected waves, window / display reflection and window / sliding door double bounces, respectively. Differences of the delay time within each sub-clusters arose mainly from whether the path experiences ceiling / floor reflection or not. We can then see that the delay spread within the sub-clusters depends on the height of the room. The higher the ceiling is, the larger the delay spread. It also depends on the relative positions of Tx and Rx within the room. Note that we cannot distinguish ceiling and floor reflection correctly due to the horizontal plane scanning of the synthetic array in the Rx side. Therefore, the DOA elevation was not considered in the clusterization procedure, otherwise the sub-clusters in cluster A might have been classified into much smaller clusters.

Cluster B has the largest number of paths among the 5 clusters. The range of the azimuth angle of arrival corresponds to the positions and size of the displays and small desks, put near the wall. Several specular diffractions from edges of the displays were detected.

Cluster C is composed of incoming signals from the Tx direction, but have longer delays. They seem to experience penetrations to and from the adjacent room. Since only two scattering points can be specified for one ray path, there is uncertainty concerning the identification of these waves and the typical paths are represented by dashed lines.

Cluster D includes several types of ray paths, i.e. ceiling reflections, floor reflections and bounces from the wooden door behind the transmitter antenna. They have the same incident azimuth angles and closer delays, which are difficult to divide into different clusters.

Cluster E consists of scattering from the walls, glass and metal frames of the slide door. As observed in cluster B, the size of the scatterer, sliding doors in this case, made the path arrival angles wider within the cluster. Here, two sub-clusters were identified.

In Table II, intra-cluster properties with respect to the first- and second-order moments are shown. Ideally the spatial and

TABLE II
INTRA-CLUSTER PROPERTIES OF THE DETERMINISTIC COMPONENTS DERIVED FROM THE LOS CHANNEL.

Cluster (Num. paths)	Angular [deg]		Delay [ns]		Mean path gain [dB]
	Mean	Spread	Mean	Spread	
A (18)	85.74	17.77	27.26	1.57	−85.21
B (33)	231.92	8.96	22.31	3.22	−83.93
C (4)	269.63	1.37	30.61	1.86	−90.36
D (22)	270.14	1.90	20.00	1.36	−83.76
E (18)	305.92	4.50	22.21	1.38	−85.21

temporal anaysis must not be carried out individually since they are highly correlated. However, the number of detected paths are too small to derive the spatio-temporal probability density functions (PDFs) within the clusters. Therefore, in this paper, the angle and delay moments were evaluated separately.

Angular spread of cluster A indicates the largest value since they contain three kinds of specular paths, as mentioned earlier. Larger angular spreads in clusters B and E confirmed the observation above that the clusters correspond to large or distributed small scattering objects. The mean received power of clusters B and D are almost the same, but the mean delay time and delay spread of cluster B are larger than those of cluster D. This is because cluster B has larger number of strong waves of double reflections than cluster D. The delay spread of cluster B shows the largest value among the 5 clusters.

D. Considerations on the Diffuse Components

The response from diffuse components (Fig. 3(b)) shows that the distribution of power on the azimuth-delay map has the same tendency with the distribution of deterministic components on its azimuth-delay map. This means that our deterministic approach could not extract power below -95 dB of the path gain sufficiently. Thus it seems that the diffuse components can be characterized from the deterministic components, but longer delayed paths whose power levels are around the floor levels (-95 dB) and appear only in the diffuse response should additionally be considered.

IV. NON-LINE-OF-SIGHT CHANNEL MEASUREMENT

A. Measurement Environment

Next, we conducted an experiment in a non-line-of-sight environment (Fig 2(b)). The previous LOS measurement was at the first floor of the house and this NLOS measurement was at the second floor, so that the size of the room was almost the same. The distance between Rx and Tx was set to 5 m, the same as the LOS measurement so that evaluation of penetration loss at the wall was possible. Specifications of the experiment and definitions of coordinates were the same as the experiment of the LOS channel. There was no furniture equipped in the room.

B. Comparison with the LOS Channel Measurement Result

Figure 5 shows the power loss of wall penetration, derived from the spectrum of shortest paths in the LOS and NLOS environments. The result is well characterized by a linear fitting in the log-scale,

$$L\ [\mathrm{dB}] = -0.3f\ [\mathrm{GHz}] - 1.8 \qquad (1)$$

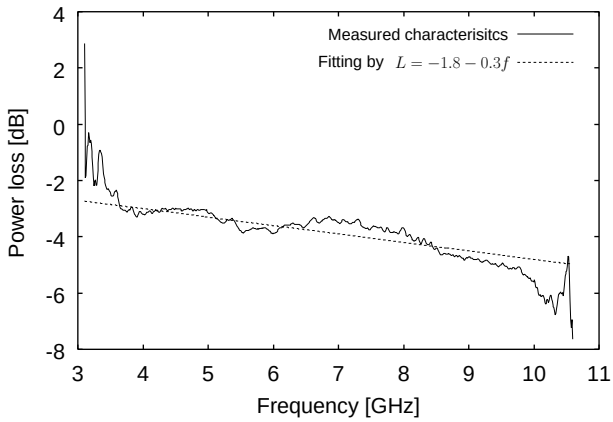

Fig. 5. Attenuation due to the wall penetration.

where L is the loss and f denotes the frequency.

In Fig. 6, two kinds of comparisons regarding the power of the extracted waves were examined. Path gain from wave #1 to #100 are shown in Fig. 6(a) and the percentage of the sum of extracted power are presented in Fig. 6(b). From these figures, it is obsereved that the detected path levels from NLOS environment were below the levels of LOS paths, mainly due to the wall penetration rather than the size of the rooms, since both measurements were conducted in rooms of the same size. Another important finding from the figures is that the propagation environment of NLOS channel is more diffuse than the LOS channel, as seen in the percentage of the sum of extracted power. In Fig. 6(b), the values from the NLOS channel is always smaller than those from the LOS channel.

C. Clusterization of the Deterministic Components

According to the clusterization by a heuristic approach, the detected deterministic components were classified into 10 clusters on the azimuth-delay map as shown in Fig. 7(a). Contrary to the LOS channel case, the number of observed clusters were much larger. What is significant in the NLOS case is that the transmitted power propagates to the receiver in a more distributed or diffuse manner. For example, cluster D consists of the shortest delay path which is equivalent to the direct path, associated with several waves whose DOAs and TOAs were around the shortest delay path. This was due to the walls, more specifically, reinforcings inside the wall. It seems to cause diffraction and produce waves around the shortest delay paths. This kind of phenomenon could not be observed in the LOS channel measurement.

It was observed that the propagating power concentrated on the specular directions in the LOS case, while they were scattered around the specular directions in the NLOS case. Therefore, the uncertainty of path identification increases in the NLOS case, especially for longer delay paths like cluster C and J. Another significant reason for this uncertainty is that only azimuthal angles were estimated in the DOD measurements and the use of a linear array resulted in an ambiguity of the angles.

Nevertheless, it can be concluded that the clusters can be attributed to the physical structures of the room even in the

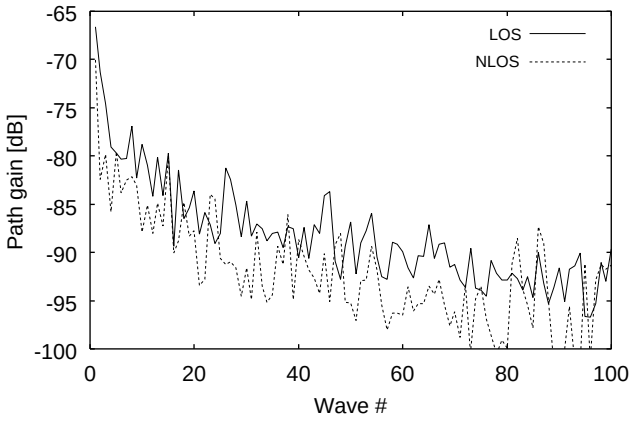

(a) Extracted power of each wave in the LOS and NLOS environment.

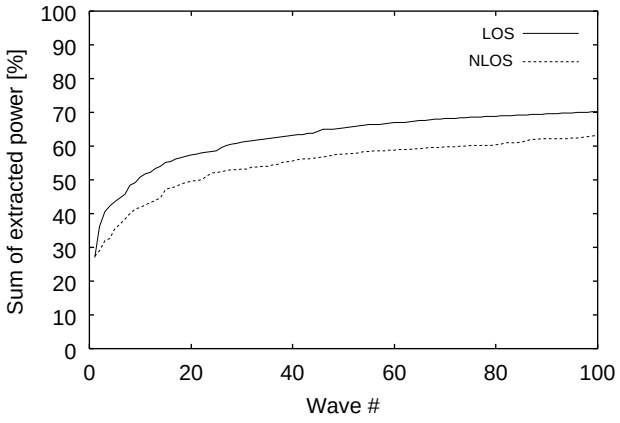

(b) Percentage of the sum of extracted power.

Fig. 6. Comparison of the LOS and NLOS measurement results in terms of power of each wave and extracted percentage of the power.

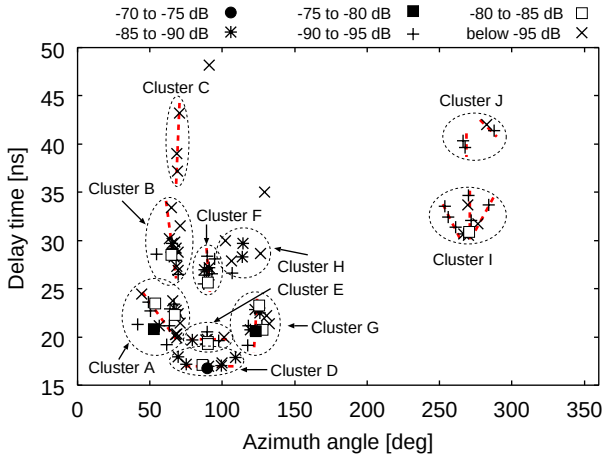

(a) Deterministic components estimated by the SAGE and their clusterization.

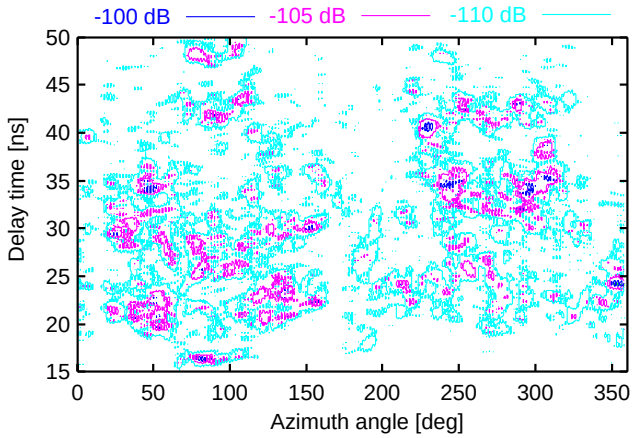

(b) Residual spectrum after the extraction of 100 waves.

Fig. 7. Separation of the deterministic components and diffuse components for NLOS channel measurement.

NLOS case as shown in Fig. 8. Clusters A, B arose from one side of the wall, while clusters G and H come from the opposite side of the wall. Clusters A and B, G and H can be distinguished by considering whether they experience a reflection from the window of Tx side or not. It is interesting to point out that although the walls were symmetric with respect to the Tx-Rx line, the number of detected paths and their power levels were slightly different. Cluster D was associated with the waves around the shortest delay paths, as explained above. Ceiling or floor reflections appeared as cluster E. The longer delay paths whose DOAs were the same as the shortest delay path correspond to the reflections from the back of the Tx, i.e. window reflections (cluster F). Clusters I and J were from the back of the Rx. Cluster I contains many specular paths and can be divided into 3 sub-clusters, while cluster J is composed of the paths which experienced multiple bounces. Note that the longest delay path (azimuth 90.8 deg, delay 48.2 ns) is assumed to experience two reflections. After penetrating the wall, it reached the window at 270° direction and then reflected at the center wall, which separates the room. Intra-cluster properties are shown in Table III.

D. Considerations on the Diffuse Components

Residual spectrum after the extraction of 100 waves in the NLOS measurement is depicted in Fig.7(b). The floor level of the spectrum was almost the same as the LOS channel case, around -100 dB with respect to the path gain, but the area of the floor level is larger than that of the LOS map. We can see that the response of the diffuse components has a relation with the power distribution of deterministic components, as suggested in the LOS case. We can still see strong responses remaining in the azimuth angle of 250° to 300° region.

TABLE III

INTRA-CLUSTER PROPERTIES OF THE DETERMINISTIC COMPONENTS DERIVED FROM THE NLOS CHANNEL.

Cluster (Num. paths)	Angular [deg]		Delay [ns]		Mean path gain [dB]
	Mean	Spread	Mean	Spread	
A (20)	56.16	6.28	22.07	1.28	−87.86
B (16)	64.98	2.44	28.95	0.98	−91.13
C (3)	69.15	0.64	39.25	2.52	−100.70
D (8)	89.39	3.96	16.84	0.21	−78.49
E (9)	89.58	3.87	19.50	0.24	−88.04
F (10)	90.12	1.81	26.52	0.83	−89.21
G (11)	123.92	2.99	21.29	1.12	−86.12
H (6)	112.74	5.04	28.61	1.11	−91.56
I (11)	269.30	5.79	31.49	1.14	−89.69
J (4)	277.54	9.84	40.87	0.82	−93.45

V. CONCLUSION

In this paper, spatio-temporal analysis of LOS and NLOS chanels based on the clusterization approach were presented. It was found that the clusters were determined by the physical structure of the environment, i.e. room height, specular directions and size of scatterers in both LOS and NLOS case, which means that the spatial and temporal channel characteristics were highly correlated. The NLOS environment was more diffuse than the LOS channel and the power propagating over the NLOS channel tends to be more distributed around the specular directions than the LOS case, due to the wall which separates the Tx and Rx. Intra-cluster properties were derived based on the moment analysis, instead of deriving a probability density function (PDF) within the clusters. The residual power spectrum after the extraction of 100 deterministic components were identified as diffuse components and their characteristics were discussed.

ACKNOWLEDGMENT

The authors would like to thank members of the NICT UWB Consortium, Akira Akeyama, Kiyomichi Araki, Fumio Ohkubo, Osamu Sasaki, Honggang Zhang, Iwao Nishiyama, Takahiro Miyamoto, Makoto Yoshikawa, and Yuko Rikuta for their help in the experiment and research.

REFERENCES

[1] K. Haneda and J. Takada, "An application of SAGE algorithm for UWB propagation channel estimation," in *Proc. IEEE Conf. on Ultra Wideband Systems and Technologies 2003 (UWBST2003)*, Reston, VA, USA, Nov. 2003.

[2] K. Haneda, J. Takada and T. Kobayashi, "Experimental evaluation of a SAGE algorithm for UWB channel sounding in an anechoic chamber," accepted for *2004 International Workshop on Ultra Wideband Systems Joint with Conference on Ultra Wideband Systems and Technologies (UWBST&IWUWBS2004)*, Kyoto, Japan, May 2004.

[3] A. Richter and R. Thomä, "Parametric modelling and estimation of distributed diffuse scattering components of radio channels," in *COST273 Temporary Documents*, TD(03)198, Prague, Czech Republic, Sept. 2003.

[4] K. Haneda, J. Takada and T. Kobayashi, "Spatio-temporal channel characterization in a home environment with ultra wideband signal," submitted to *Intl. Conf. on Wireless Personal Multimedia Communications 2004 (WPMC04)*, Padova, Italy, Sept. 2004.

[5] Federal Communications Commission, "Revision of part 15 of the commission's rules regarding ultra-wideband transmission systems," in *Final Report and Order*, FCC 02–48, Apr. 2002.

[6] T. Taniguchi and T. Kobayashi, "An Omni-directional and low-VSWR antenna for the FCC-approved UWB frequency band," in *Proc. 2003 IEEE AP-S Int. Symp. (AP-S '03)*, pp. 460–463, Ohio, USA, June 2003.

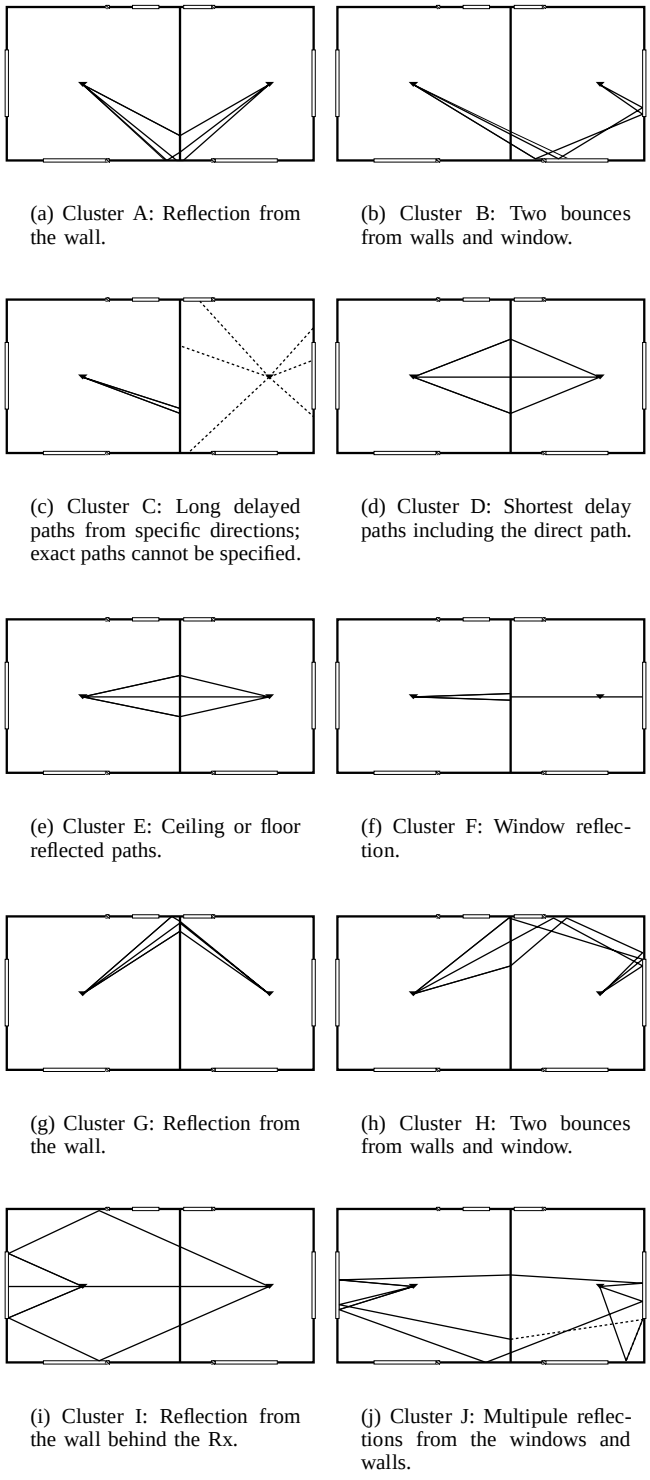

(a) Cluster A: Reflection from the wall.

(b) Cluster B: Two bounces from walls and window.

(c) Cluster C: Long delayed paths from specific directions; exact paths cannot be specified.

(d) Cluster D: Shortest delay paths including the direct path.

(e) Cluster E: Ceiling or floor reflected paths.

(f) Cluster F: Window reflection.

(g) Cluster G: Reflection from the wall.

(h) Cluster H: Two bounces from walls and window.

(i) Cluster I: Reflection from the wall behind the Rx.

(j) Cluster J: Multipule reflections from the windows and walls.

Fig. 8. Cluster identification with respect to physical structures of the environment for the NLOS channel measurement. Typical paths are also shown.